Evaluation of the Function exp(x^2) erfc(x) to Higher Precisions for Higher Order Derivative Polarography of CE-type Electrode Process

Myung-Hoon Kim*, Veriti P. Smith, and Tae-Kee Hong+

Alfriend Chemical Laboratory, Department of Chemical Science, Old Dominion University, Norfolk, Virginia 23529 U.S.A. *Received March 9, 1990*

The function exp(x^2) erfc(x), which is often encountered in studies of electrode kinetics, is evaluated to an extended precision with 32 significant decimal digits in order to find theoretical relationships used in derivative polarography/voltammetry for a chemically-coupled electrode process. Computations with a lower precision are not successful. Evaluation of the function is accomplished by using three types of expansions for the function. Best ranges of arguments are selected for each equation for particular precisions for efficiencies. The method is successfully applied to calculate higher-order derivatives of the current-potential curves in all potential ranges for a reversible electron transfer reaction coupled with a prior chemical equilibrium (*i.e.*, a CE type process). Various parameters that characterize the peak asymmetry (such as ratios of peak-heights, ratios of half-peak-widths, and separations in peak-potentials) are analyzed to find how kinetic and thermodynamic parameters influence shapes of the derivatives. The results from the CE process is compared with those from an EC process in which a reversible electron transfer is coupled with a follow-up homogeneous chemical reaction. The two processes exibit quite contrasting differences for values of the parameters.

Introduction

It has been suggested in recent years that polarographic current-potential curves can be more precisely analyzed if one takes derivatives of the potential-current curves and then examine several variables that are associated with the derivative curves[1,2]. However, there are several problems associated with the derivative approach in both computational and experimental aspects. This paper deals with a problem in the computational aspects.

Although most scientific computations can be handled with double-precision arithmetic (typically 14 to 16 decimal digits) when single-precision arithmetic (typically 6 to 9 decimal digits) yields inaccurate results, some computations which are encountered in chemistry in recent years cannot be adequately handled even with the double-precision mode. For example, it has been shown that concentration-distance profiles and current-potential-time relationships under certain polarographic/voltammetric conditions can be found only through a higher precision computation requiring about 30 decimal digits[1]. Moreover, the problems associated with the level of precision become especially serious in the derivative approach of polarography[2,3], where evaluations of current derivatives include subtraction involving two terms of comparable magnitude, hence generating severe round-off errors. The error becomes a serious matter in a progressive manner as the order of differentiation increases.

The functional form of exp(x^2)erfc(x) occurs frequently as a solution or as a part of a solution for current expressions of many electrochemical boundary value problems whenever diffusion is coupled with a slower chemical or electrochemical kinetic step[4]. This is true regardless of the methods employed[4,5]: such methods include polarography/voltammetry, chronoamperometry, and chronocoulometry. One of the simplest and most popular ways to evaluate the function is based on Hasting's rational approximations of the error function[6,7]. However, the earlier rational approximations for erf(x) or erfc(x) are strictly limited to single-precision with absolute errors being larger than 1×10^{-7} in general[8]. For more accurate evaluations of the functions, more rigorous rational approximations with higher degree polynomials[9] or approximations with several types of truncated series expansions for the function[10] have been employed. Reports on the evaluation and analysis of the function exp(x^2)erfc(x) have previously appeared in several journals[11-14]. Oldham's report[12] on an algorithm which is suitable for a microcomputer is based on a combination of several types of expansions including a continued fraction expansion of the function. Commercial software packages are also available for mainframe-computers[15] and also for microcomputers[16]. However, all previous reports and the commercial packages for the functions are strictly limited to lower precision (double or below), and they are not suitable for computations requiring high accuracy for the functional values. Thus, the aims of this paper are (a) to present an effective algorithm for the evaluation of the function beyond double-precision to quadruple-precision with 32 decimal significant figures, and (b) to apply the algorithm to calculate theoretical values of derivatives for a chemically coupled electrode process (CE-type) then analyze the asymmetry found in derivative peaks to extract thermodynamic and kinetic information on the CE system. The algorithm is primarily for main-frame computers where the word length is larger (64 bits or above), but it will be suitable for future microcomputers since microcomputers with 64-bit devices do not seem too far away to advent.

Precision of experimental polarograms is limited typically to a half precision (3–5 significant decimal figures) as in most of other common scientific measurements. It has been well-known that differentiation of such experimental data is a noise-enhansing procedure by its nature; this raises a serious question about how peractical the derivative approach can be. However, recent microprocessor-controlled commercial electrochemical instruments (from such companies as EG & G Princeton Applied Research, Bioanalytical Systems, Inc.,

+ Visiting Scholar from Department of Chemistry, Hanyang University, Seoul 133-791, Korea

IBM, and Cypress Systems, Inc.) or similar types of instruments provide better signal-handling capabilities (such as signal-averaging, signal-smoothing and differentiation); the digital signal output enables one to obtain the derivative polarogram/voltammogram with a good signal-to-noise (S/N) ratio more easily than those obtained with analog instruments in earlier days. Examples of first and second derivative polarograms obtained from such a digital instrument (BAS 100) can be found from references (2) and (3), in which the derivatives are generated from a numerical differentiation coupled with a moving-window-average method, although the derivatives are somewhat distorted from true derivatives. The distortion of signals can be eliminated if the software is improved[3]. In this studies[2], three different types of digital-filtering methods (*i.e.*, the moving-window-average method (MWM), the Savitzky-Golay method (SGM, a floating least-squares method) and a fast Fourier transformation method (FFT) are compared; the SGM with a multiple pass appears to be more satisfactory than the MWM in obtaining second derivatives because signal distortions with the SGM is much less than those with the MWM. Details of the studies is presented elsewhere[2]. Future development of algorithms for the smoothing/differentiation method should yield noise-free third derivatives if noises are not too high (noises being less than 1% of a signal).

Methods

The evaluations of the function are based on the three types of series expansions of the function which have been commonly used[10] for more rigorous treatments of the function. It utilizes a power series expansion for lower values of arguments, an asymptotic expansion for higher values of arguments, and an continued fractional expansion for moderate to higher values of the argument. In principle, the algorithms are similar to those used to evaluate the series to lower precision. However, the range of valid arguments for the three forms of expansions for required precision, and the extent of summations or inclusions of fractional terms for the expansions should be very different from those for lower precisions.

The power series for smaller arguments[10] is

$$\begin{aligned}&\exp(x^2)\mathrm{erfc}(x)\\&=\exp(x^2)[1-2/\pi^{1/2})\exp(-x^2)\\&\quad\sum_{n=0}^{\infty}\{2^n/1\cdot3\cdot\cdots(2n+1)\}x^{2n+1}]\\&=\exp(x^2)-(2/\pi^{1/2})[x+(2/3)x^3+(4/15)x^5\\&\quad+(8/105)x^7+\cdots]\end{aligned}\tag{1}$$

The asymptotic expansion for larger arguments[17, 10] is

$$\begin{aligned}&\exp(x^2)\mathrm{erfc}(x)\\&\cong[1/(\pi^{1/2}x)]\sum_{n=0}^{n}\{(2n-1)!!/(-2x^2)^n\}\\&=[1/(\pi^{1/2}x)][1-1/(2x^2)+3/(4x^4)-15/(8x^6)\\&\quad+105/(16x^8)-\cdots]\end{aligned}\tag{2}$$

Table 1. Number of Terms Required in Each Expansion to Meet the Precision at Selected Values of the Argument

Precision (Digits)	Eqn.	$x=1.5$ (1)	(3)	(2)	$x=6.0$ (1)	(3)	(2)	$x=10.0$ (1)	(3)	(2)
Half (3-4)		13	12	—	108	3	3	—	3	3
Single (7-8)		17	32	—	115	8	12	—	4	5
Double (16)		25	105	—	129	14	35	—	10	11
Triple (24)		30	193	—	130	26	—	—	16	23
Quadruple (32)		38	374	—	130	40	—	—	24	41

The expression for the continued fraction expansion[10] is

$$\exp(x^2)\mathrm{erfc}(x)=\frac{(2/\pi)^{1/2}}{2^{1/2}x+}\,\frac{1}{2^{1/2}x+}\,\frac{2}{2^{1/2}x+}\,\frac{3}{2^{1/2}x+}\cdots\tag{3}$$

First, the efficiency of the three equations for the evaluation of the functions at the required precisions are examined in order to find a best algorithm that can minimize CPU time. This is done by checking how many terms are necessary for the evaluation at a requried precision level for each expansion at selected values of the argument. Typical results at several selected values of the arguments are summarized in Table 1. As in the case for lower precision, eqn. (1) is most effective at a small argument ($x=1.5$) for higher precision as well. For example, eqn. (1) is approximately 10 times faster than eqn. (3) for quadruple precision since it needed to sum only the first 38 terms to reach the required precision with eqn. (1) as compared to needing the first 374 terms with the eqn. (3). Eqn (2) is totally inadequate to use at $x=1.5$. At a moderate value of argument ($x=6.0$), eqn. (1) is the most inefficient because it needed as many as 108 terms just to attain half precision, although the required number of terms for higher precision does not increase very rapidly (*e.g.*, 130 terms for quadruple precision). Equations (3) and (2) are comparably good for lower precision at $x=6.0$; however, only the continued fractional expansion (eqn. (3)) is a viable expression at higher precisions for $x=6.0$. At this value of x, the asymptotic expansion (eqn.(2)) is of no use for quadruple-precision, because the smallest absolute value of a term in the expansion never reaches 10^{-32} which is the error for the precision. At larger values of the argument ($x=10$), both eqns. (2) and (3) are comparably efficient at levels of all precision, while eqn. (1) is totally unsatisfactory at any precision.

Based on analyses which are similar to those above, ranges of arguments for which each equation can be effectively handled with the fewest terms for the various levels of precision are searched, and the results are given in Table 2. The values at the limits of the ranges of the argument are chosen so that number of terms included in both equations become comparable. For example, to triple-precision, both eqns (1) and (3) require 59 terms for $x=3.0$; therefore $x=3.0$ defines the range limit when determining which equation to choose. All other range limits were determined based on the similar criteria. Eqn. (3) is not effective at moderate or large values of the argument. On the other hand, eqn. (2) cannot be used for high precision at moderate values of the argument ($5<x<8.6$). Eqn. (2), however, is as effective as the eqn. (3) for larger values of the argument at any level of precision. The numbers in parentheses in Table 2 are the maximum

Table 2. Ranges of the Argument for which Each Equation is Efficient for the Evaluation of the Function at the Stated Level of Precision. The Maximum Number of Terms Required at Particular Levels of Precision in Each Expansion is Given in Parentheses

Precision (# digits)	Relative Error	Eqn. (1) Power Series	Eqn. (3) Fractional	Eqn. (2) Asymptotic
Half (3-4)	10^{-3}-10^{-4}	$0<x<1.5$ (13)	$1.5<x$ (12)	$3.5<x$ (12)
Single (7-8)	10^{-7}-10^{-8}	$0<x<2.0$ (24)	$2.0<x$ (21)	$4.5<x$ (20)
Double (16)	10^{-16}	$0<x<2.5$ (40)	$2.5<x$ (40)	$8.5<x$ (14)
Triple (24)	10^{-24}	$0<x<3.0$ (59)	$3.0<x$ (59)	$10<x$ (23)
Quadruple (32)	10^{-32}	$0<x<3.5$ (74)	$3.5<x$ (82)	$20<x$ (19)

number of terms used in the expansion for the given ranges of the argument at the particular levels of precision. Values of the function are computed with an algorithm based on Table 2.

Typical results are presented in the following to 32 digits at several selected values of the argument ranging widely from 10^{-10} to 10^{+10}.

x	exp(x²)erfc(x)
10^{-10}	: 0.99999999988716208330044874260963
10^{-5}	: 0.99998871630832829262648294464597
10^{-1}	: 0.89645697996912664193188374864404
1	: 0.42758357615580700441075034449057
2	: 0.25539567631050574386508858091080
10	: $0.56140992743822585857517387220468 \times 10^{-1}$
10^{+5}	: $0.56418958351954680777492305908892 \times 10^{-5}$
10^{+10}	: $0.56418964132077555819267566199529 \times 10^{-10}$

The calculations described here were carried out on an IBM 4381/3090 with VM/CMS operating system with an extended precision (32 digits) mode. Plotting of the current-potential curves and their derivatives (Figure 1, 2, and 4) are accomplished by using the FPS plotting software with a Zeta 836 high performance digital plotter (Nicolet). The three-dimensional graphs (Figure 3) are generated with a software Surfer (Version 3.00, Golden Software).

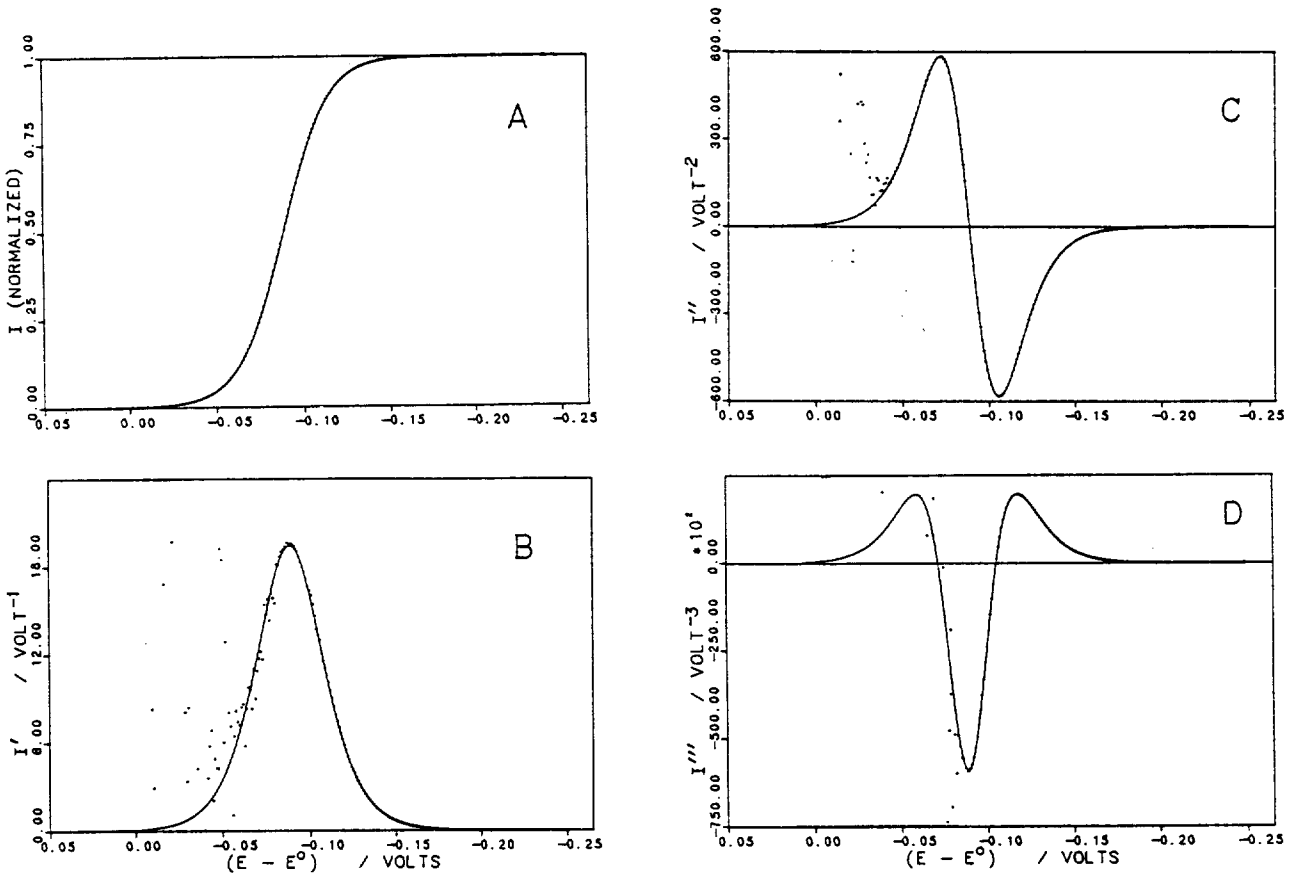

Figure 1. (A) Normalized current and (B) its first derivative *vs.* potential curves for a C_rE_r process with $K_{eq}=10^{-3}$, $k_f=10^{+7}$, $n=2$, and $T=298$ K. Dots represent the results from single-precision computation; solid lines represent result from double-precision computation. (C) The second derivative and (D) the third derivative of the normalized current *vs.* potential curves for the C_rE_r process: dots represents results from double-precision computation, and solid lines represent quadruple-precision results. Data are presented in a potential range from +0.01 V to −0.25 V. Data from the lower precision calculations in the anodic end (+0.05 to +0.01 V) of the potentials are not presented in the figures; but those data, with value outside the plotting range, are the worst in fact in terms of error.

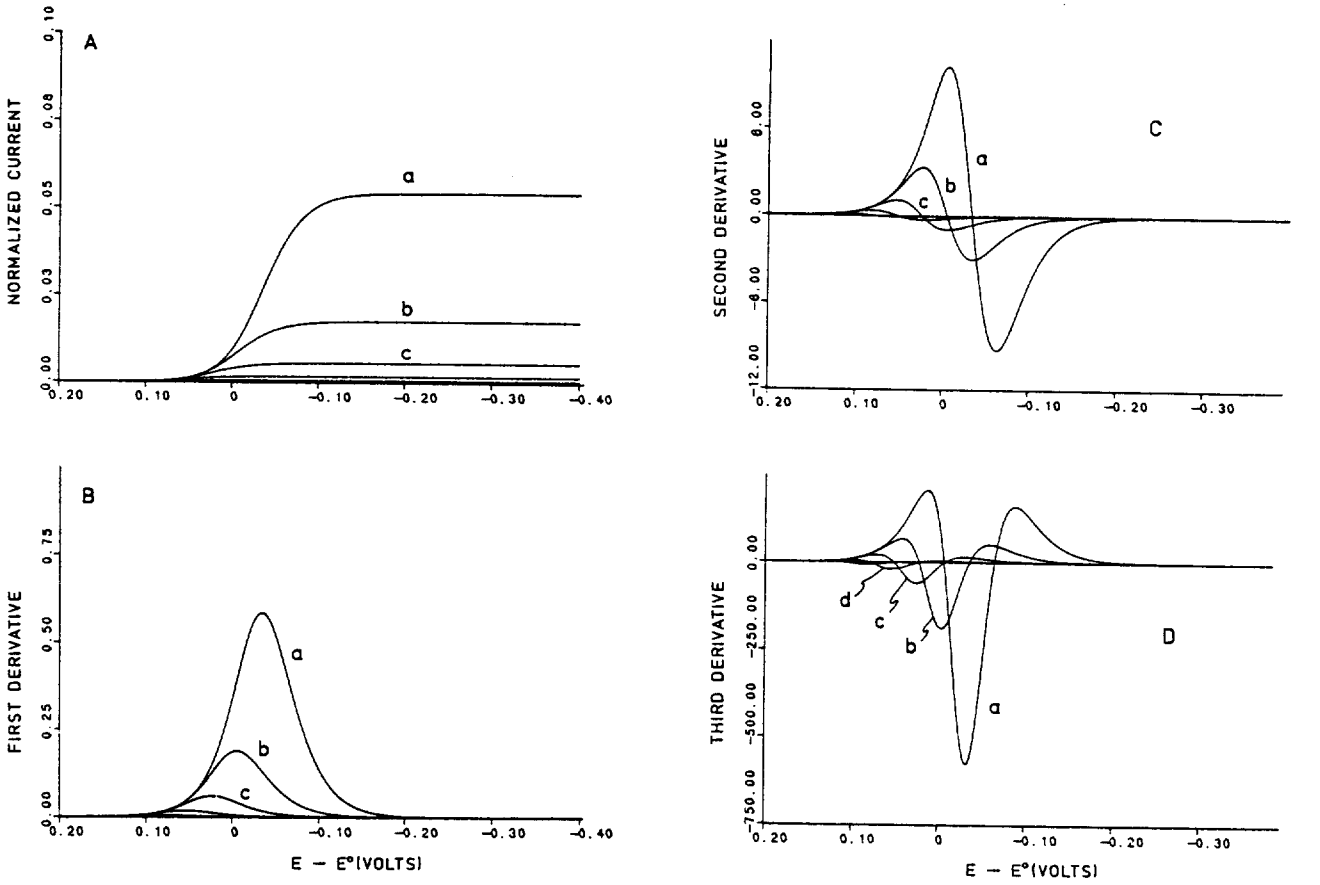

Figure 2. (A) The Normalized current, (B) their first, (C) second, and (D) third derivative at various values of the forward rate constant (k_f) at $K_{eq} = 10^{-4}$ for the CE-type of electrode process; $k_f = 10^{-1}s^{-1}$ (a), 10^{-2} (b), 10^{-3} (c), 10^{-4} (d), and 10^{-5} (e). Calculated for $T = 298$ K, $t = 1.0$ s, and $n = 1$.

Results and Applications

Evaluation of the function with above method is applied to the theoretical computation for the current-potential relationship and its derivatives for a chemically-coupled electrode process. A reversible electron transfer reaction coupled with a prior chemical equilibrium (*i.e.*, C_rE_r type electrode process) can be represented as follows:

$$Y \underset{k_b}{\overset{k_f}{\rightleftharpoons}} O \quad K_{eq} = [O]/[Y] = k_f/k_b \text{(in solution)} \tag{4}$$

$$O + ne^- \longrightarrow R \quad \text{Nernstian (at the electrode)} \tag{5}$$

Current (i) as a function of an applied potential (E) for this system under a linear diffusion condition can be given by the following equations (5, 18):

$$i = i_d[(\pi t K_{eq} k_f)^{1/2} \exp\{K_{eq} k_f((1+\in)/K_{eq})^2 t\} \operatorname{erfc}\{(K_{eq} k_f)^{1/2}(1+\in)/K_{eq} t^{1/2}\}] \tag{6}$$

where, $i_d = nFAD^{1/2}C/(\pi t)^{1/2}$ (7)

$$\in = \exp[(nF/RT)(E - E_{1/2})] \tag{8}$$

F is the Faraday constant, A is an area of an electrode surface, D is the diffusion coefficient of the species O, C is the bulk concentration of Y and O, t is the time at which the current is sampled after application of the potential, and $E_{1/2}$ is the reversible polarographic half-wave potential of O. Expressions for the current can be simplified by putting

$$x = (K_{eq} k_f)^{1/2}[(1+\in)/K_{eq}] t^{1/2} \tag{9}$$

Then, $i = i_d[(\pi t)^{1/2}(K_{eq} k_f)^{1/2} \exp(x^2) \operatorname{erfc}(x)]$ (10)

An analytical differentiation of eqn. (10) with respect to the applied potential (E) gives

$$i' = i_d(nF/RT)(2k_f t) \in [(1+\in/K_{eq})i - 1] \tag{11}$$

Further differentiations of eqn. (11) yields second and third derivatives

$$i'' = i_d(nF/RT)^2(2k_f t) \in [(1+\in/K_{eq})i + RT/nF(1+\in/K_{eq})i' - 1] \tag{12}$$

$$i''' = i_d(nF/RT)^3(2k_f t) \in [(1+4\in/K_{eq})i + (2RT/nF)(1+2\in/K_{eq})i' + (RT/nF)^2(1+\in/K_{eq})i'' - 1] \tag{13}$$

From the expressions, current and its derivatives are calculated with values of $K_{eq} = 10^{-3}$, $k_f = 10^{+7}$, $n = 2$ and $T = 298$ K at various levels of precision. Comparison of the results from single- and quadruple-precisions are given in Figure 1 for the original current (A) and its first derivative (B). Solid

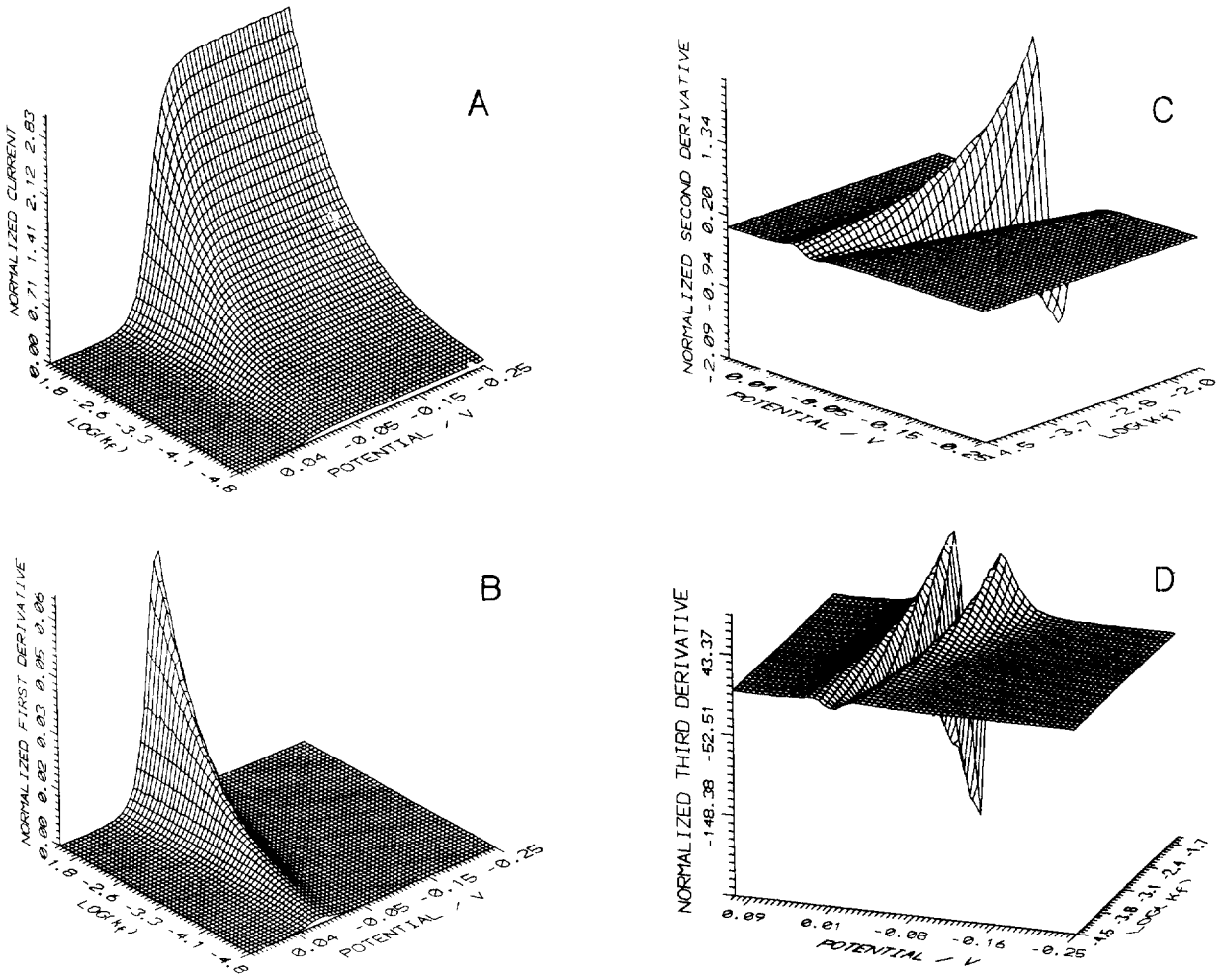

Figure 3. Three-dimensional plots of (A) the normalized current, (B) their first, (C) second, and (D) third derivatives as a function of potential and forward rate constant (k_f) at $K_{eq} = 10^{-4}$. The perspectives of the second (C) and third (D) derivatives are different from those of the zeroth (A) and first (B) derivatives, and it was chosen for a better view of the valleys present in the second and the third derivaties. Conditions are same as in Figure 3.

lines are from the quadruple-precision computation, and dots are from the single-precision. There are not any significant differences in the original currents (Figure 1A) for the results using the two levels of precision. However, the single-precision computation did not produce a satisfactory result for the first derivative of the anodic half of the peak (Figure 1B). The single-precision computations is totally unable to produce a satisfactoy second and third derivatives. In other words, the single-precision computation yielded erroneous results for the first, second and third derivatives when $x>800$, $x>20$, and $x>11$, respectively. With a double-precision computation the second and third derivatives become erroneous for $x>8{,}000$ and $x>300$ respectively, which is usually the case when larger values of k_f is employed in the anodic end of the potential range. It should be pointed out that errors arise from the terms inside the brackets in eqn. (11)-(13), which inevitably involve round-offs during the subtractions. Any dots with values outside the plotting scales (for example, 0.0-24.0 for Figure 1B) on y-axis of the figures are forced to be located at the rim of the figure boxes for the calculation with lower precisions. Therefore, the actual errors are much larger than those which appear in the figures. In general, the more anodic (positive) the potentials are, the larger the errors are, although it does not appear so from the figure; namely, errors appear largest in the middle (-0.01 to -0.04 V) of the anodic side of the potential range. This is because data are presented only in the potential range but from +0.01 to -0.25 V, not from +0.05 to -0.25 V. It looks that it is error-free in the range from +0.05 V to +0.01 V; but, in fact, this anodic end is the worst range in terms of error. Figure 1C and 1D depict the second and the third derivatives under the same conditions at two levels of precision. Solid lines are from the quadruple-precision computation and dots are from a double-precision computation for the same system. Please note the heavy scattering of the points at the anodic branches of the two curves. As the system becomes relatively slower ($k_f<10^{+4}$), the errors due to the use of lower precision diminish. The evaluation is not successful with the double-precision especially in the anodic branch of the third derivative because the values of the argument of the function in the potential range become so large ($x>500$). A very similar type of the error for derivative-potential curves is also observed with another kinetic system[2a], *i.e.*, a

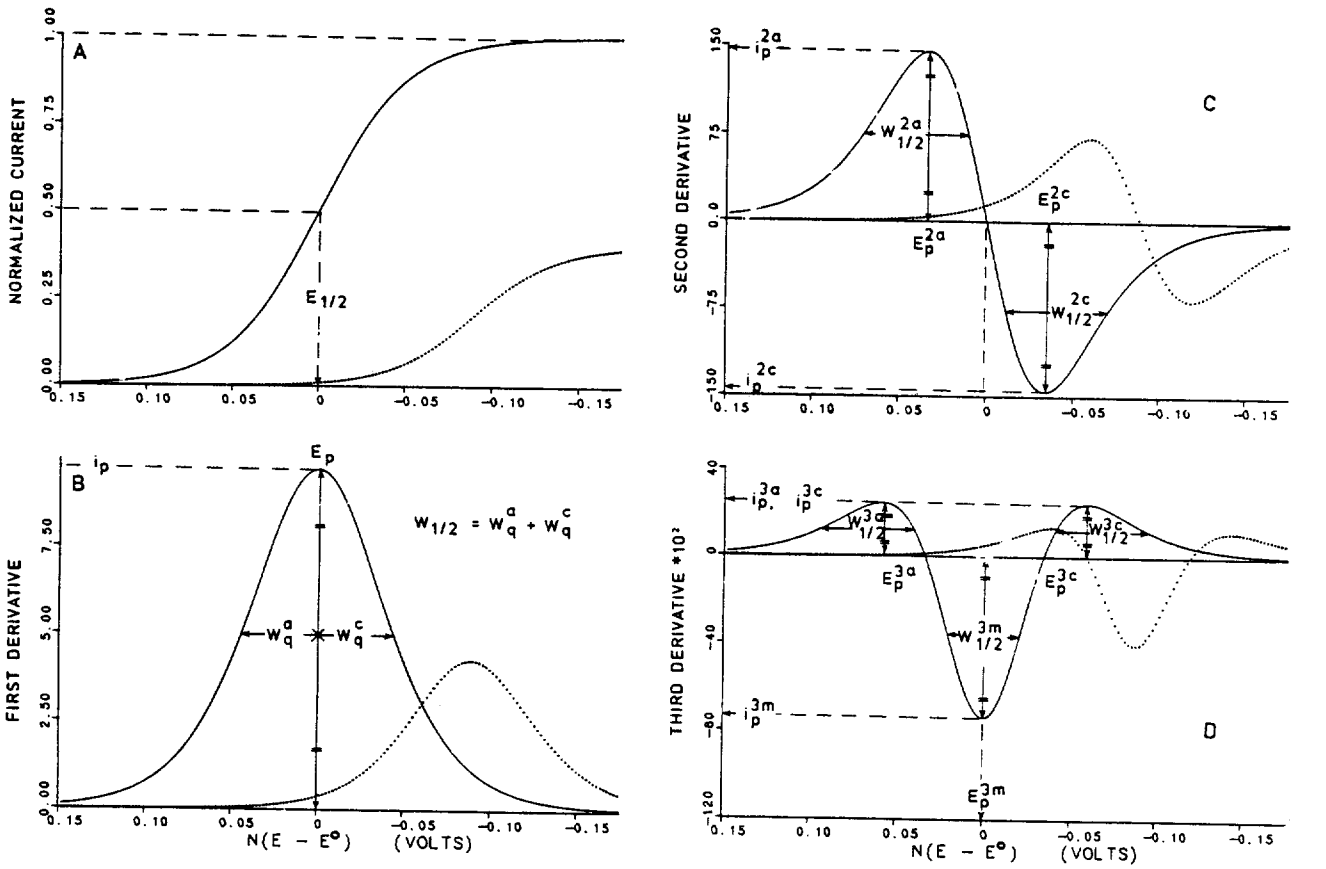

Figure 4. (A) Normalized current-potential curves, (B) its first, (C) second, and (D) third derivatives for a reversible electron transfer reaction (solid lines) and for the CE-type reaction (dots). Graphic representations for various parameters are also given. Potentials are with respect to the formal potential, E^o, hence $E_{1/2}$. Calculated for $T = 298$ K, and $t = 1.0$ sec.

quasi-reversible process with higher values of the transfer coefficient ($\alpha > 0.8$): the errors for this system can also be corrected by using the high precision level computation. Details of the study on the quasi-reversible and irreversible systems will be presented elsewhere[2a].

The current as a function of the potential and the forward rate constant (k_f) at a given value of the equilibrium constant ($K_{eq} = 10^{-4}$) for the homogeneous chemical step are depicted in Figure 2. A three-dimensional view of the graphs are presented in Figure 3 for a better overview of picture. The derivatives can be analyzed in terms of various parameters as defined in Figure 4. The parameters defined are various peak-potentials (E_p's), peak-heights (i_p's), and half-peak widths ($W_{1/2}$'s): the numeric superscripts in the parameters stands for an order of the differentiation, while the alphabetic superscripts (*a*, *m*, and *c*) stand for anodic, middle, and cathodic, respectively. Close examinations of the derivatives reveals asymmetry associated with the peaks for the CE system. The presence of the asymmetry is not too apparent in the zeroth (Figure 2A and 3A), first (Figure 2B and 3B), and second derivatives (Figure 2C and 3C); but it is readily noticeble in the third derivative (Figure 2D and 3D), namely, the anodic-peak-currents (i_p^{3a}) are higher than the cathodic-peak-currents (i_p^{3c}). The analysis of lower order (the first and second) derivatives for the C_rE_r process is already presented elsewhere[3]. In this work, analysis of the third derivative will be presented bacause the asymmetry found in the third order derivative is more pronounced and more sensitive to kinetics than that found in the second- and lower-order derivatives.

Analysis of Peak-Potentials and Their Separations. Figure 5A shows a plot of three peak-potentials (E_p^{3a}, E_p^{3m} and E_p^{3c}) of the third derivatives as a function of k_f at the two different values of K_{eq} (10^{-2} and 10^{-4}). All three peak-potentials shift towards positive direction as the value of the forward rate constant increases, which is the same trend as observed for the peak-potential of the first and second derivatives. Separation of the peak-potentials, (E_p^{3a}-E_p^{3c}), (E_p^{3a}-E_p^{3m}), and (E_p^{3m}-E_p^{3c}), are presented in Figure 5B. As the forward rate constant of the prior chemical step becomes smaller, they decreases from the values of the simple reversible electrode process. (E_p^{3a}-E_p^{3c}) decreases from 118 mV to 90 mV exhibiting most changes (28 mV), while (E_p^{3a}-E_p^{3m}) decreases from 59 mV to 51 mV exhibiting least changes (8 mV). (E_p^{3m}-E_p^{3c}) decreases from 59 mV to 41 mV with a net change of 18 mV. It should be noted that the change associated with the anodic branch (E_p^{3m}-E_p^{3a}) is more sensitive to than that with the cathodic branch (E_p^{3m}-E_p^{3c}).

Analysis of Peak-Heights. Three peak-heights (i_p^{3a}, i_p^{3m}, and i_p^{3c}) for the third derivatives are normalized with respect to values of three peak-heights for the reversible process, then plotted against $\log(k_f)$ in Figure 6A. All three peak-heights decreases as the forward rate constant decreases for all values of K_{eq}, which is an analogous behavior to that of the second and first derivatives. The normalized anodic-peak-heights are always larger than the cathodic ones.

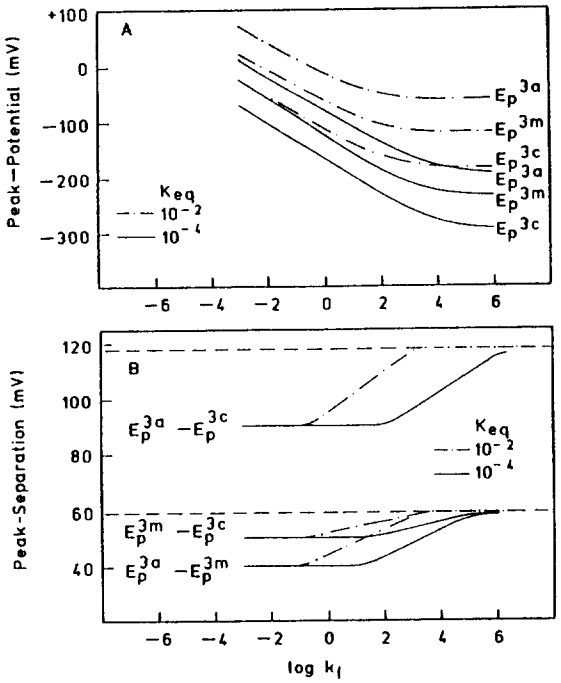

Figure 5. Effect of the forward rate constant, k_f, (A) on the anodic-, middle- and cathodic-peak-potentials (E_p^{3a}, E_p^{3m}, and E_p^{3c}) of the third derivative, and (B) on the separations in the peak potentials (E_p^{3a}-E_p^{3c}, E_p^{3a}-E_p^{3m}, and E_p^{3m} E_p^{3c}) at two different values of K_{eq}(= 10^{-2} and 10^{-4}). Calculated for T = 298 K, and t = 1.0 sec.

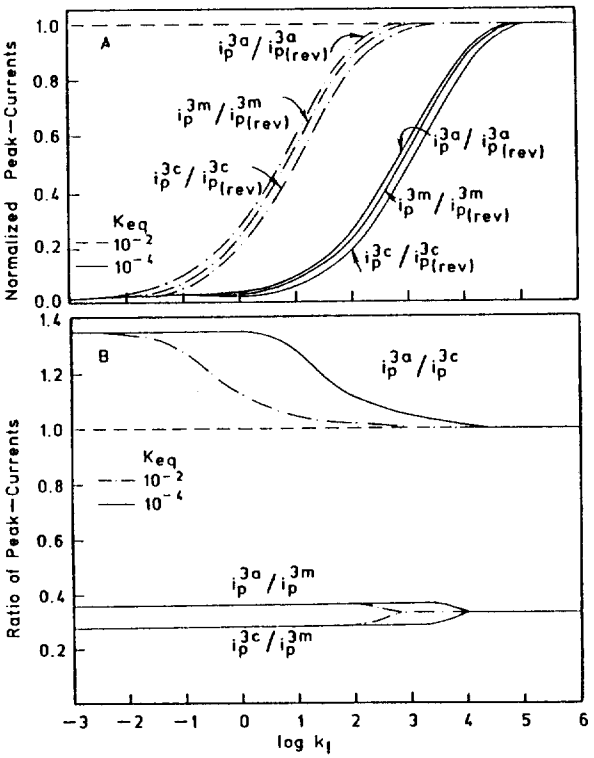

Figure 6. (A) Effect of the forward rate constant, k_f, on the heights of the anodic, middle, and cathodic peaks (i_p^{3a}, i_p^{3m}, and i_p^{3c}) at two different values of the equilibrium constant. Values of the heights are normalized with respect to those of the reversible cases. Conditions are same as in Figure 5. (B) Effect of k_f on the various ratios of the peak-heights (i_p^{3a}/i_p^{3c}, i_p^{3a}/i_p^{3m}, and i_p^{3m}/i_p^{3c}).

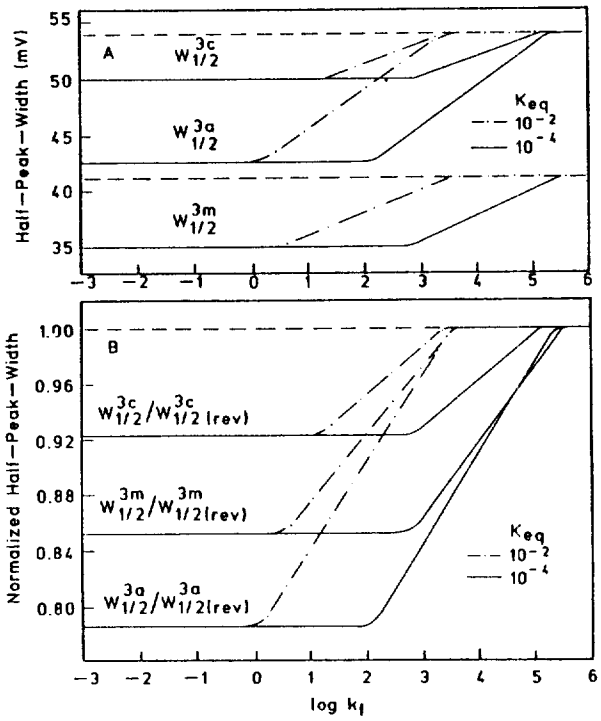

Figure 7. Effect of the forward rate constant, k_f, (A) on the anodic, middle, and cathodic half-peak-widths ($W_{1/2}^{3a}$, $W_{1/2}^{3m}$, and $W_{1/2}^{3c}$) of the third derivative, and (B) on their counterparts normalized against their reversible values at the two different values of the equilibrium constant. Conditions are same as in Figure 5.

Therefore, the ratio of the anodic-to-cathodic peak-heights are always larger than 1. Three ratio of the peak-heights (namely, i_p^{3a}/i_p^{3c}, i_p^{3a}/i_p^{3m}, and i_p^{3m}/i_p^{3c}) as a function of k_f are given in Figure 6B for the two values of the equilibrium constant. As k_f decreases, the ratio of the anodic-to-cathodic peak-height increases from the reversible value of 1.0 to 1.35: this 35% change the ratio is substantial enhancement from 25% change in the ratio observed from the second derivative at the same condition[3]. It is interesting to note that the ratio of the anodic-to-middle peak-height increases from the reversible value of 0.32 while that of the cathodic-to-middle peak-height decreases.

Analysis of Half-Peak-Widths. Absolute value of three half-peak-widths ($W_{1/2}^{3a}$, $W_{1/2}^{3m}$, and $W_{1/2}^{3c}$) for the third derivatives as a function of log(k_f) is presented in Figure 7A. All three peaks become sharper as k_f decreases. The anodic ($W_{1/2}^{3a}$) and cathodic ($W_{1/2}^{3c}$) half-peak-width decrease from 54 mV to 42.5 mV and 50 mV respectively, while the middle half-peak-widths ($W_{1/2}^{3m}$) decreases from 41.2 mV to 35 mV. The anodic-half-peak-widths become sharper than the cathodic ones. The absolute values of the half-peak-widths are normalized against those of their reversible counterparts, and the results are given in Figure 7B. The anodic half-peak-width exhibits most changes (by 22%), while the cathodic half-peak-width produce least changes (only by 8%) from the reversible value of unity. The middle one shows about 15% decrease. The various ratios of the half-peak-widths (*i.e.*, $W_{1/2}^{3c}/W_{1/2}^{3a}$, $W_{1/2}^{3a}/W_{1/2}^{3m}$, and $W_{1/2}^{3c}/W_{1/2}^{3m}$) are presented in Figure 8. As k_f decrease, the cathodic-to-anodic half-peak-width increases to a limiting value of 1.17 from 1.00 (the reversible value). The anodic-

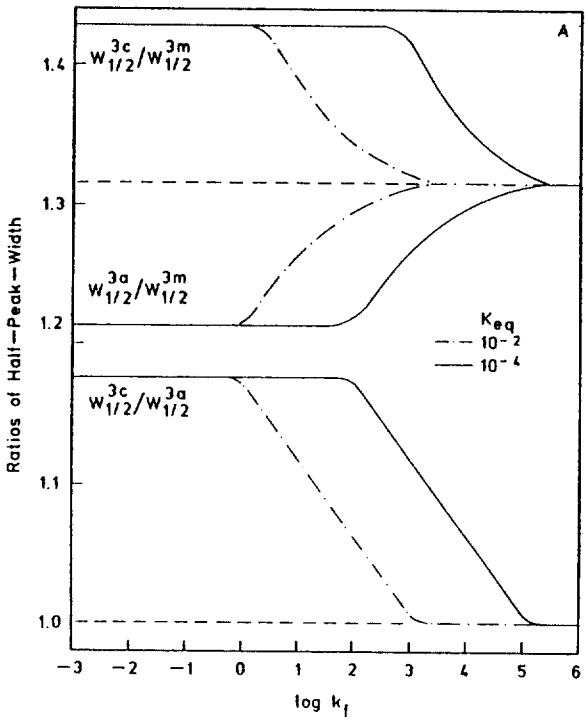

Figure 8. Effect of the forward rate constant, k_f, on the various ratios of half-peak-widths ($W^{3c}_{1/2}/W^{3a}_{1/2}$, $W^{3a}_{1/2}/W^{3m}_{1/2}$, and $W^{3c}_{1/2}/W^{3m}_{1/2}$) at two different values of the equilibrium constant. Conditions are same as in Figure 5.

to-middle half-peak-width decreases to 1.21 from 1.31, while cathodic-to-anodic half-peak-width increase 1.43 from 1.31 that is the value for the reversible process. It should be pointed that relative changes in the cathodic-to-anodic half-peak-width for the third derivative is more than that for the second derivative although their behavior is similar.

In general, *the effect due to the coupled kinetics on the parameters are more sensitively reflected in the third derivative than in the lower-order (namely, second and first) derivatives.* As observed in the second derivative, all parameters associated with the anodic peak (E^{3a}_p, i^{3a}_p, and $W^{3a}_{1/2}$) are more strongly influenced by the preceeding homogene ous chemical step than their cathodic counterparts (E^{3c}_p, i^{3c}_p, and $W^{3c}_{1/2}$). Comparisons of various diagnostic parameters from all derivatives are made and summarized in Table 3 for the reversible, the CE-type, and EC-type processes[2(b)]. Values of many parameters (such as ratios of peak-heights, and ratios of half-peak-widths) of the CE-type process change from the reversible values in opposite direction to the values for the EC-type process, although some parameters (such as peak-separations) changes in a same direction for both CE and EC processes. In other words, the anodic-to-cathodic peak-height ratio for the CE-type process is less than one (the reversible value), while that for EC-type process is larger than one. However, a peak separation (E^{3a}_p-E^{3c}_p), exhibits a same behavior for both CE- and EC- type processes becoming less than 118/n mV which is for the reversible process. Therefore, all the peak-current ratios and half-peak-width ratios can be used as diagnostic parameters for distinguishing a CE from an EC mechanism because they exhibits opposite behaviors, while the various peak-separations cannot be used for the diagnostic purpose because they change in a same manner.

Table 3. Comparison of Values of Various Diagnostic Parameters for the Reversible, CE and EC Processes for T = 298 K, and = 1.0 sec

Parameters	Reversible	C_rE_r Process	E_rC_i Process
Original current			
$E_{1/4}-E_o$	= 0.0 mV	<0.0 mV	>0.0 mV
$E_{1/4}-E_{3/4}$	= 56.4/n mV	<56.4/n mV	<56.4 mV
1st derivative			
E_p-E^o	= 0.0 mV	<0.0 mV	>0.0 mV
i_p/i_d	= 9.7	<9.7	>9.7
$W_{1/2}$	= 90.5/n mV	<90.5/n mV	<90.5/n mV
W^a_q/W^c_q	= 1.0	<1.0	>1.00
2nd derivative			
$E^{2a}_p-E^{2c}_p$	= 68.0/n mV	<68.0/n mV	
$i^{2a}_p-i^{2c}_p$	= 1.0	>1.0	<1.00
$W^{2a}_{1/2}-W^{2c}_{1/2}$	= 1.00	<1.0	>1.00
3rd derivative			
$E^{3a}_p-E^{3c}_p$	= 118/n mV	<118/n mV	<118/n mV
$E^{3a}_p-E^{3m}_p$	= 59/n mV	<59/n mV	<59/n mV
$E^{3m}_p-E^{3c}_p$	= 59/n mV	<59/n mV	<59/n mV
$i^{3a}_p-i^{3c}_p$	= 1.00	>1.00	<1.00
$i^{3a}_p-i^{3c}_p$	= 0.32	>0.32	<0.32
$W^{3a}_{1/2}-W^{3c}_{1/2}$	= 0.32	<0.32	>0.32
$W^{3a}_{1/2}-W^{3m}_{1/2}$	= 1.00	<1.00	>1.00
$W^{3c}_{1/2}-W^{3c}_{1/2}$	= 1.31	<1.31	>1.31
$E^{2a}_p-E^{2c}_p$	= 1.31	>1.31	<1.31

Acknowledgement. This work is supported partially by the Academic Computing Service of Old Dominion University, and by NSF with the computer time made available through the Cornell National Supercomputing Facility. The author thanks Drs. John D. Van Norman, Andrzej Lasia and Robert L. Ake for helpful discussions and reading the manuscript. Part of the results were presented at the 3rd Chemical Congress of North America, Toronto, Canada, June, 1988 and at the 23rd Meeting of the Analytical Division of the Korean Chemical Society, Hanyang University, Seoul, Korea, July 19, 1988.

REFERENCES

1. M.-H. Kim, *Anal. Chem.*, **59**, 2136-2144 (1987).
2. (a) M.-H. Kim and V. P. Smith, *J. Electroanal. Chem.*, Submitted for publication (1989); (b) M.-H. Kim, *J. Electrochem. Soc.*, **137**, 3815-3825 (1990).
3. M.-H. Kim and V. P. Smith, *Anal. Sci. Tech.*, **2**, 225-245 (1990).
4. A. J. Bard and L. R. Faulkner, Electrochemical Methods, John Wiley & Sons, New York, p. 166, 205 and p. 274, 1980.
5. D. D. Macdonald, Transient Techniques in Electrochemistry, Plenum Press, New York, p. 78, 98, and pp. 156, 1977.
6. C. Hastings, Jr., Approximations for Digital Computers,

Princeton University Press, Princeton, New Jersey, 1955.
7. M. Abramowitz and I. Stegun, Handbook for Mathematical Functions, National Bureau of Standards, Washington, D.C., Chap. 7, 1964.
8. J. F. Hart, *et al.*, Computer Approximations, SIAM Series in Appl. Meth., Wiley, New York, 1968.
9. W. J. Cody, *Mathematics of Computation*, **23**, 631–637 (1969).
10. J. Spanier, J. and K. B. Oldham, An Atlas of Functions, Hemisphere Publishing Co., Washington, Chapt. 41, 1987.
11. K. B. Oldham, *Mathematics of Computation*, **22**, 454 (1968).
12. K. B. Oldham, *J. Electroanal. Chem.*, **136**, 175–177 (1982).
13. K. B. Oldham and R. A. Osteryoung R. A., *J. Electroanal. Chem.*, **11**, 397 (1966).
14. R. de Levie, *J. Electroanal. Chem.*, **170**, 387–389 (1984).
15. IMSL, SFUN/LIBRARY, IMSL, Houston, Texas, pp. 3–10, 1984.
16. W. H. Press, B. P. Flannery, S. A. Teukolsky, and W. T. Vetterling, Numerical Recipes, Cambridge University Press, Cambridge, p. 163, 1986.
17. M. L. Boas, Mathematical Methods in the Physical Sciences, 2nd Ed., John Wiley & Sons, New York, pp. 467–471, 1983.
18. M.-H. Kim and R. L. Birke, *Anal. Chem.*, **55**, 1735–1741 (1983).

Enhanced Electrogenerated Chemiluminescence of Tris (2,2′-bipyridyl) Ruthenium (II)–$S_2O_8^{2-}$ System by Sodium Dodecyl Sulfate

Sung Chul Kang, Sooil Oh, and Kang-Jin Kim*

Department of Chemistry, Korea University, Seoul 136-701. *Received April 25, 1990*

The electrochemical reduction and electrogenerated chemiluminescence (ECL) of $Ru(bpy)_3^{2+}$–$S_2O_8^{2-}$ in CH_3CN–H_2O solution were studied in the presence of sodium dodecyl sulfate (SDS) as an anionic surfactant. SDS enhanced the ECL and the fluorescence intensities and lengthened the duration of ECL due to the solubilization of reactants and possibly to the stabilization of ECL intermediates in the SDS micellar environment.

Introduction

Interests in the electrogenerated chemiluminescence (ECL) of tris(2,2′-bipyridyl) ruthenium(II)($Ru(bpy)_3^{2+}$) in aqueous or acetonitrile–water solutions have been increasing rapidly since $Ru(bpy)_3^{2+}$ as an ECL label can be used to determine low concentrations of biologically important compounds.[1,2] In particular, the ECL mechanism of $Ru(bpy)_3^{2+}$–$S_2O_8^{2-}$ system in acetonitrile–water solution estabilished recently by White and Bard are based on the following reaction sequence.[2]

$$Ru(byp)_3^{2+} + e^- \rightarrow Ru(bby)_3^{+} \quad (1)$$

$$Ru(bby)_3^{+} + S_2O_8^{2-} \rightarrow Ru(bpy)_3^{2+} + SO_4^{\cdot-} + SO_4^{2-} \quad (2)$$

$$Ru(bpy)_3^{+} + SO_4^{\cdot-} \rightarrow Ru(bpy)_3^{2+*} + SO_4^{2-} \quad (3)$$

Because $Ru(bpy)_3^{+}$ is unstable in aqueous solutions and $S_2O_8^{2-}$ has a low solubility in CH_3CN solutions[3], the CH_3CN–H_2O mixed solutions are used to produce intense ECL emission.

Electrogenerated reactive intermediates are often stabilized in micellar media on the reductive electrochemical system. For example, Saveant *et al.*[4] have reported a remarkable stabilization of the electrogenerated anion radical of phthalonitrile in the presence of cationic micelles and suggested that the observed 250 fold decrease in the rate of protonation of the anion radical was due to its association with the positively charged micelles. On the other hand, Blount *et al.*[5] found that anionic micelles in the presence of LiCl electrolyte were capable of stabilizing the nitrobenzen anion radical to the point where it become detectable by cyclic voltammetry at 50 mV/sec.

Recently, Ouyang and Bard[6] examined the oxidative electrochemistry and ECL of $Os(bpy)_3^{2+}$, and suggested that $Os(bpy)_3^{2+}$ interacted most strongly with anionic micelles, and both the electrochemical response and ECL in the presence of oxalate were suppressed. Bard and coworkers[7] had previously shown that the anionic micelles associated more strongly with methylviologen cationic radical(MV^{+}) than the dication (MV^{2+}) form and $Ru(bpy)_3^{2+}$ is bound into Nafion more strongly than $Ru(bpy)_3^{3+}$. Their results were explained by the hydrophobic interactions between the given substrate and the micellar hydrocarbon core or the nonpolar regions of Nafion.

However, micellar systems have not been utilized for the ECL of $Ru(bpy)_3^{2+}$–$S_2O_8^{2-}$ system, although there are some reports concerning the CL improvements of lucigenin in micelle solutions.[8,9] Therefore, in this paper we attempt to describe the effect of sodium dodecyl sulfate (SDS) as an anionic surfactant for the purpose of enhancing the ECL efficiency of $Ru(bpy)_3^{2+}$–$S_2O_8^{2-}$ system. Possible causes of the enhancement are discussed.